

# Occurrence of two quantum critical points in $\text{Yb}_2\text{Pd}_2\text{Sn}$ or, Yb systems do not behave mirror-like to Ce compounds

E. BAUER<sup>\*</sup>, H. MICHOR, T. MURAMATSU<sup>a</sup>, T. KANEMASA<sup>a</sup>, T. KAGAYAMA<sup>a</sup>, K. SHIMIZU<sup>a</sup>, Y. AOKI<sup>b</sup>, H. SATO<sup>b</sup>, M. GIOVANNINI<sup>c</sup>

*Institute of Solid State Physics, Wiedner Hauptstrasse 8-10, Vienna University of Technology, A-1040 Wien, Austria*

<sup>a</sup>*Kyokugen, Center for Quantum Science and Technology under Extreme Conditions, Osaka University, Toyonaka, Osaka 560-8531*

<sup>b</sup>*Department of Physics, Tokyo Metropolitan University, Tokyo 192-0397, Japan*

<sup>c</sup>*Dipartimento di Chimica e Chimica Industriale, University of Genova, Via Dodecaneso 31, I-16146 Genova*

We report on the discovery of two pressure driven quantum critical points appearing in ternary  $\text{Yb}_2\text{Pd}_2\text{Sn}$ , where the application of pressure of about 1 GPa establishes long-range antiferromagnetic order, but above an upper bound of about 4 GPa, magnetic order vanishes again, giving rise to two phase transitions at zero temperature. Associated with the QCP's in  $\text{Yb}_2\text{Pd}_2\text{Sn}$ , we observe nFI behaviour from precise resistivity measurements. We argue that this emergent behaviour corresponds to two pressure dependent, mutually competing energy scales exerted to the Yb ions. Electronic properties associated with the paramagnetic state below and above the critical pressures disagree, as evident from a negative and a positive Grüneisen parameter, respectively. Our novel finding, without much doubt, is a unique property of Yb systems.

(Received April 1, 2008; accepted June 30, 2008)

**Keywords:** Pressure driven critical points, Yb-Pd-Sn, Quantum phase transition

## 1. Introduction

Unlike thermal phase transitions, where a characteristic order parameter is driven by thermal fluctuations from the ordered to the disordered state (or vice-versa), quantum phase transitions are a consequence of quantum fluctuations. The latter may be fine-tuned by externally applied pressure, magnetic fields or even by substituting or doping certain elements in a given material. Such procedures allow to continuously change a thermal – towards a quantum phase transition. Several intermetallic compounds and oxides have been studied so far in great detail, proving that these particular systems are driven across a quantum critical point (QCP), where a magnetic phase transition is approached virtually at zero temperature as the consequence of a subtle balance of two competing ground states. Right there, many extraordinary, phenomena like unconventional superconductivity or non-Fermi-liquid (nFI) features may occur [1–4].

Landau's Fermi liquid theory effectively describes metals at low temperatures, providing, in general, simple power laws for the temperature dependence of physical quantities such as the electrical resistivity ( $\rho \propto T^2$ ), the electronic contribution to the specific heat ( $C_e \propto T$ ) or the Pauli susceptibility ( $\chi_{\text{Pauli}} = \text{const.}$ ). In Yb (or Ce) intermetallic compounds a Fermi liquid ground state

appears in case of weak magnetic Yb (or Ce) intersite interactions as a consequence of heavy quasi-particle formation due to the coherent Kondo interaction of conduction electrons and localized Yb(Ce)-4f moments. Thereby all Yb(Ce)-4f magnetic degrees of freedom are bound in Fermi liquid ground state. Among materials, where electron interactions are intensely, systems with a subtle balance between on-site Kondo interactions (defining the Kondo scale TK), and inter-site magnetic coupling (constituting TRKKY) are of particular importance because of the possibility of a  $T = 0$  magnetic phase transition. Such a phase transition is triggered by quantum fluctuations exuding into an extended phase space. This provokes a breakdown of Fermi liquid predictions, manifested by temperature dependencies of physical quantities, which sharply differ from the simple power laws indicated above, giving rise to a new state of matter, the *non-Fermi liquid* (nFI).

A quantum critical point (QCP) is usually the endpoint of a line of continuous finite-temperature transitions tuned by various control parameters, i.e., pressure, magnetic fields or substitution. While phase transitions at finite temperatures may be always accounted for by a classical description, the critical fluctuations at a QCP require a quantum-statistical description. The latter, however, corresponds to the former via an effective dimensionality,  $d_{\text{eff}} = d + z$ , where  $d$  is the dimensionality of the system and

$z$  the dynamical exponent, with  $z > 1$  for metallic magnetic systems.

Within the preceding decade various materials have been studied in detail, with  $\text{Ce}(\text{Cu},\text{Au})_6$  being a prototypic series. A magnetic phase transition at  $T = 0$  and, associated, nFL properties have been found via the application of pressure, magnetic fields and substitution [5]. Some of such systems, e.g.,  $\text{CeCu}_2\text{Ge}_2$  [6],  $\text{CeRhIn}_5$  [7], and  $\text{CeRhSi}_3$  [8], even show unconventional superconductivity, once the finite magnetic phase transition is driven against zero.

Yb compounds, on the contrary, are assumed to behave in many respects mirror-like to Ce systems, causing that e.g., the magnetic state of the Yb ion becomes stabilized by pressure. This means that non-magnetic Yb

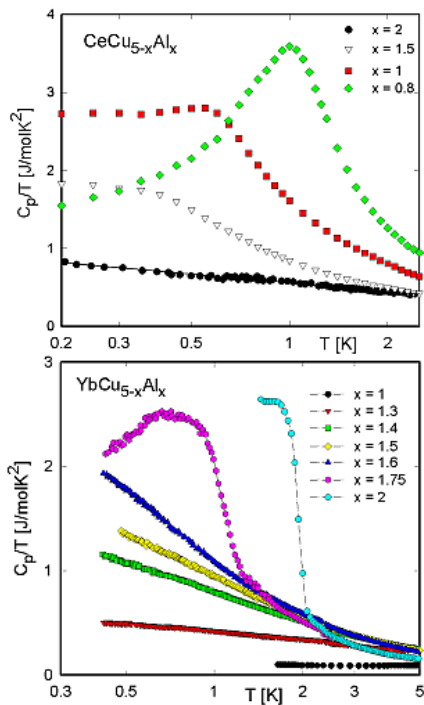


Fig. 1. Temperature dependence of the specific heat  $C_p$  plotted as  $C_p/T$  vs.  $\ln T$  of  $\text{CeCu}_{5-x}\text{Al}_x$  (upper panel) and  $\text{YbCu}_{5-x}\text{Al}_x$  (lower panel) revealing nFL features near critical concentrations  $x \approx 2$  (Ce) and  $x \approx 1.5$  (Yb).

Systems can be driven towards a magnetic instability. Some examples here are:  $\text{YbCu}_2\text{Si}_2$  [9, 10],  $\text{YbNi}_2\text{Ge}_2$  [11],  $\text{Yb}_2\text{Ni}_2\text{Al}$  [12] and  $\text{YbCuAl}$  [13].  $\text{YbRh}_2\text{Si}_2$  [14], just by chance, is in the proximity of its QCP, already at ambient pressure.

## 2. Results and discussion

To illustrate the mirror-like behaviour of isomorphous cerium and ytterbium compounds, hexagonal  $\text{CeCu}_{5-x}\text{Al}_x$

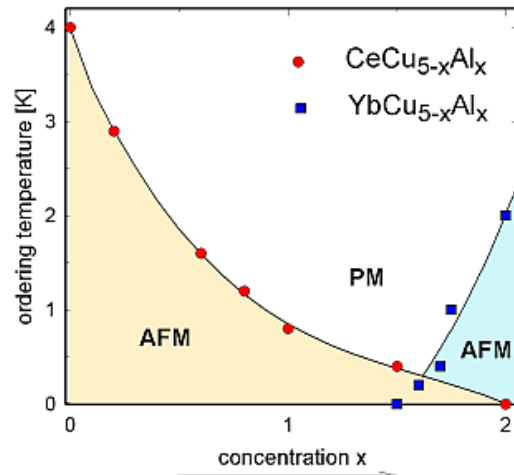


Fig. 2. Magnetic phase diagram of  $\text{cecu}_{5-x}\text{al}_x$  and  $\text{ybcu}_{5-x}\text{al}_x$ .

and  $\text{YbCu}_{5-x}\text{Al}_x$  compounds are selected. Both series of compounds allow a substitution of 2 Cu atoms by Al. Following the very general observation that Ce compounds containing  $3d$  elements with filled  $d$  shells result in a magnetic ground state, while Yb compounds containing the same partner elements add up to a nonmagnetic ground state,  $\text{CeCu}_5$  orders magnetically below  $T_N = 4$  K [15], but  $\text{YbCu}_5$  stays non-magnetic due to the almost divalent state of the Yb ion [ $v(\text{YbCu}_5) \approx 2.2$ ] [16]. This is clearly reflected from specific heat data collected for both series of compounds (compare Fig. 1). Substituting Cu/Al dramatically modifies the ground states of both series. Increasing Al content suppresses long range magnetic order in case of the Ce series, but above  $x \approx 1.5$  long range magnetic order is established in  $\text{YbCu}_{5-x}\text{Al}_x$ . The latter results from an increase of the Yb valency, approaching  $v \approx 3$  around  $x = 1.5$ . Right at that critical concentration, non-Fermi liquid features are observed, as documented e.g., by the logarithmic contribution to the heat capacity. For the Ce based series, a quantum critical point is approached for  $\text{CeCu}_3\text{Al}_2$ .

In terms of Kondo interaction present in both series of compounds, again a counter-trend is observed: increasing Al in the Ce based series drives an increase of  $T_K$ , thus the RKKY interaction becomes outbalanced; as a consequence long range magnetic order vanishes at the critical concentration  $x \approx 2$ . In the case of the Yb based series,  $T_K$  decreases as the Al content grows, resulting in a magnetic instability at  $x \approx 1.5$ .

Previously performed investigations of both series allow to establish the respective phase diagram as plotted in Fig. 2. This prototypic behaviour deduced would justify the frequently used picture of the mirror-like behaviour of Ce and Yb compounds as a consequence of the electron-hole analogy of both elements.

The present paper aims to demonstrate that Yb systems are unique in various aspects by showing that pressure applied to Yb compounds may result in the occurrence of two quantum critical points. Such an

unparalleled and novel feature is not expected to happen in any material based on  $\text{Ce}$ .

The subject of the present study is  $\text{Yb}_2\text{Pd}_2\text{Sn}$ , a ternary  $\text{Yb}$  system which crystallises in the tetragonal  $\text{Ho}_2\text{FeB}_2$  structure (lattice parameters:  $a = 0.758$  nm and  $c = 0.364$  nm) with space group  $D_{4h}^5$ . Alternating layers of  $\text{Yb}$  and another of  $\text{Pd}$  and  $\text{Sn}$  stack sequentially along the  $c$ -axis. The  $4h$  site occupied by  $\text{Yb}$  has a low  $mm$  point symmetry. Physics of  $\text{Yb}_2\text{Pd}_2\text{Sn}$  is controlled by the non-integer valent state of the  $\text{Yb}$  ion, corresponding to a valence  $v \approx 2.9$  [17]. Since  $(\text{Yb}_2\text{Pd}_2\text{Sn}) < 2.95$ , a magnetic instability at finite temperatures is rather unlikely. Magnetic order of  $\text{Yb}$  systems requires valencies of the  $\text{Yb}$  ions very close to the  $3+$  state [16]. As accomplished above, the proximity of the present  $\text{Yb}$  compound to the  $3+$  state and thus to a magnetic electronic configuration may give rise to unconventional ground state features at ambient pressure. This apparently follows from heat capacity and electrical resistivity data taken at low temperatures.

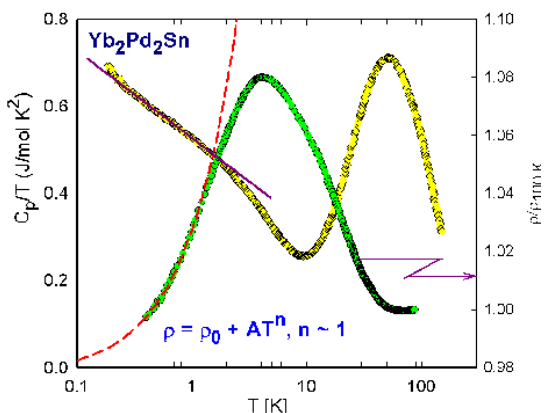


Fig. 3. Temperature dependence of the specific heat  $C_p$  (left axis) and of the electrical resistivity (right axis) of  $\text{Yb}_2\text{Pd}_2\text{Sn}$  plotted on a logarithmic temperature scale. The heat capacity is displayed as  $C_p/T$  which at low temperatures renders the electronic contribution; the almost logarithmic dependence below 2 K is emphasized by a solid line. The low temperature behaviour of  $\rho(T)$  is approached by a power law with  $\rho(T) = \rho_0 + AT^n$ , where  $\rho_0$  is the residual resistivity,  $A$  is a material dependent constant and  $n \approx 1$  (dashed line), implying a nFL behaviour.

Results are shown in Fig. 3. The specific heat  $C_p$  of  $\text{Yb}_2\text{Pd}_2\text{Sn}$  is plotted as  $C_p/T$  vs.  $T$  and refers to the left axis of this figure. Two distinct features at low temperatures are remarkable:

i) The large values of  $C_p/T$  indicate a strongly renormalized density of states right at the Fermi-energy as a consequence of a pronounced Kondo type interaction between the conduction electron spin and the  $\text{Yb-4f}$  moments. ii) The almost negative logarithmic temperature dependence below about 2 K and extending over one order of magnitude down to about 200 mK is an unambiguous

signature of a non-Fermi liquid state of  $\text{Yb}_2\text{Pd}_2\text{Sn}$  at low temperatures and ambient pressure. The latter conclusion is backed by measurements of the electrical resistivity,  $\rho$ , in the low temperature region (compare Fig. 3). Data are plotted on a logarithmic temperature scale and refer to the right axis of this figure. The overall behaviour is reminiscent of a Kondo lattice, where the maximum at low temperature constitutes the energy scale,  $T_K$  of the system. At low temperatures  $\rho(T)$  behaves roughly linearly, inferring that the system significantly deviates from a Fermi liquid behaviour ( $\rho \propto T^2$ ) as expected for ordinary metals at low temperatures. This observation is in line with the present heat capacity data, evidencing the nFL state adopted by  $\text{Yb}_2\text{Pd}_2\text{Sn}$ .

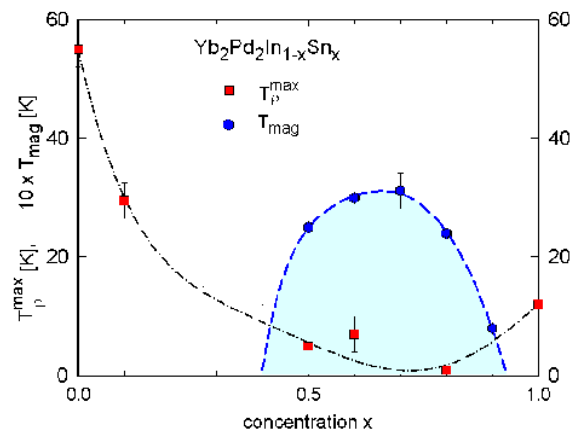


Fig. 4. Phase diagram of  $\text{Yb}_2\text{Pd}_2\text{In}_{1-x}\text{Sn}_x$ . The hatched area represents the phase space of the antiferromagnetically ordered regime of this series. The filled squares are the respective temperatures of the low temperature maxima in  $\rho(T)$ , with  $T_{\rho}^{\max} \propto T_K$ . The blue circles are the magnetic ordering temperatures  $T_{\text{mag}}$ .

$\text{Yb}_2\text{Pd}_2\text{Sn}$  is the end member of a series of substituted compounds, starting with non-magnetic  $\text{Yb}_2\text{Pd}_2\text{Sn}$ , where the In/Sn substitution unexpectedly triggers magnetic order in a narrow concentration range of Sn-rich compounds [17]. Ordering, however, occurs only in that range where the respective volumes of the unit cells adopt minima values, in other words, where chemical pressure acts onto the  $\text{Yb}$  ions. Here,  $\text{L}_{\text{III}}$  spectroscopy indicates that the valence of the  $\text{Yb}$  ions attains  $v = 3$  [17]. A tentative phase diagram regarding the exceptional behaviour of magnetic ordering is sketched in Fig. 4.

Besides the magnetic ordering temperature as deduced from specific heat and resistivity measurements as well as from neutron elastic scattering, the temperature of the resistivity maximum, with  $T_{\max} \rho \propto T_K$  [18], is shown in Fig. 4, too. This extraordinary observation in the context of a recent theoretical proposition that pressure tunes the parameter  $R = T_{\max} \rho / T_K$  of  $\text{Yb}$  systems in a unique manner [19] motivated a high pressure study of  $\text{Yb}_2\text{Pd}_2\text{Sn}$  using a diamond anvil cell [20], where resistivity measurements were performed down to the mK range.

Many microscopic measurements concerning the valence of Yb compounds (e.g. L<sub>III</sub> absorption edge data) have shown that the application of pressure tunes the valence of Yb from a certain intermediate stage towards the magnetic 3+ state for reasonable large values of pressure. As an example it is mentioned that a pressure of about 20 GPa exerted to YbCu<sub>5</sub> varies the valency of Yb from  $v \approx 2.2$  ( $p = 1$  bar) to  $v \approx 3$  [21]. In this context, one would expect that pressure about one order of magnitude smaller should be sufficient to drive Yb<sub>2</sub>Pd<sub>2</sub>Sn into the proximity of the 3+ state, where a magnetic instability may be observed.

Figs. 5(a,b) display the temperature dependent resistivities of Yb<sub>2</sub>Pd<sub>2</sub>Sn for various pressures applied. In accordance to the ambient pressure results, low temperature maxima are obvious from the pressure dependent study. In general, such maxima are a consequence of coherence, separating the single-ion Kondo regime ( $T > T_{\rho}^{\max}$ ) from the regime, where coherent Kondo scattering dominates ( $T < T_{\rho}^{\max}$ ) may be considered as being proportional to the Kondo temperature  $T_K$  [18]. Increasing pressure, however, changes the overall character of  $\rho(T)$ , since the pronounced maximum

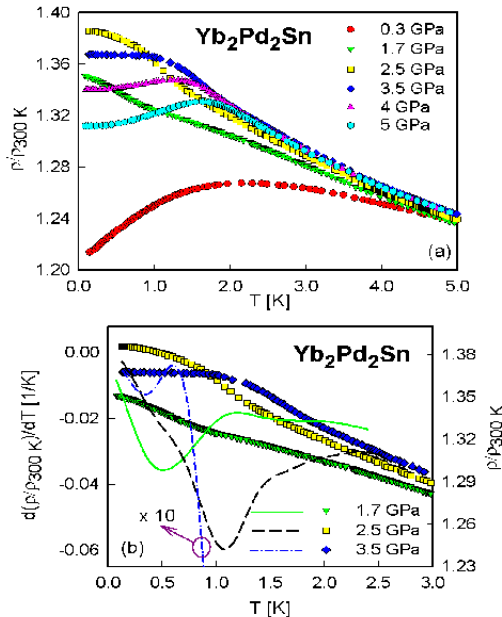


Fig. 5. (a) Temperature dependent electrical resistivity of Yb<sub>2</sub>Pd<sub>2</sub>Sn at various pressures, normalized to room temperature. At ambient pressure  $\rho(300K) \approx 90 \mu\Omega\text{cm}$ . Data for  $p=0.3$  GPa are shifted by 0.05 upwards. (b) Low temperature derivative  $d\rho/dT$ .

vanishes, but in turn a shoulder-like structure develops. A closer inspection of these data based upon a  $d\rho/dT$  plot evidences distinct anomalies provoked by a magnetic phase transition. This conclusion is theoretically corroborated by Fischer et al. [22], revealing

$d\rho/dT \propto C_{mag}(T)$ . It is well known that  $C_{mag}(T)$  right at the magnetic phase transition temperature holds a typical anomaly and thus serves to establish the onset of long range magnetic order.

Such anomalies are found 0.91 and 1.23 K for 1.7 and 2.5 GPa, respectively, as well as at 0.45 K for 3.5 Pa (compare Fig. 5(b)). We also note that similar features are obvious from resistivity measurements of Yb<sub>2</sub>Pd<sub>2</sub>(In, Sn) for those concentrations, where long range magnetic order is observed [17]. We therefore conclude that the anomaly in  $\rho(T,p)$  is associated with magnetic ordering at  $T_N$ , triggered by the emergence of the full trivalent state of Yb under compression of the unit cell volume. The enhancement of the resistivity below  $T_N$  indicates so-called superzone boundary effects, where a gap opens in the DOS since the magnetic Brillouin zone may differ from the electronic one [23]. At  $p = 2.5$  GPa we have applied various magnetic fields (Fig. 6, upper panel) which demonstrate that i) fields below 3 T quench magnetic

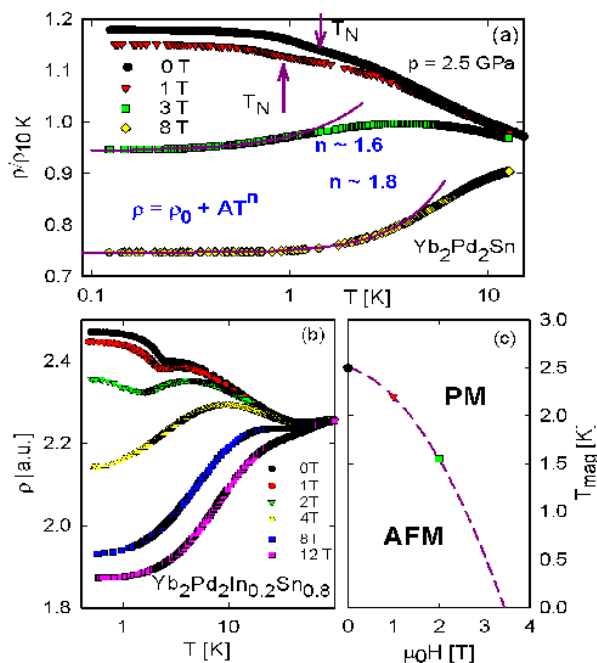


Fig. 6. (a) Normalised temperature dependent resistivity  $\rho$  of Yb<sub>2</sub>Pd<sub>2</sub>Sn at  $p = 2.5$  GPa for various values of external magnetic fields. The solid lines are least squares fits (see the text) and the arrows indicate the magnetic phase transition temperatures. (b) Normalised temperature dependent resistivity  $\rho$  of Yb<sub>2</sub>Pd<sub>2</sub>In<sub>0.2</sub>Sn<sub>0.8</sub> for various values of external magnetic fields. (c) Magnetic phase diagram of Yb<sub>2</sub>Pd<sub>2</sub>In<sub>0.2</sub>Sn<sub>0.8</sub>

order, being indicative of an antiferromagnetic state, while ii) a simple power law behaviour develops for  $\rho(T)$  near to the critical field with  $\rho(T) \propto T^{1.6}$ . An increase of the field to 8 T reveals  $n \approx 1.8$ , signifying that the system mutates from the nFl towards the Fermi liquid state owing to suppression of spin fluctuations by the applied field.

Interestingly, the field response of  $\text{Yb}_2\text{Pd}_2\text{In}_{0.2}\text{Sn}_{0.8}$  (Fig. 6, lower panel) shows about the same features: bulk magnetic order, evidenced by the sharp anomaly at  $T = T_N$  becomes suppressed as the magnetic field strength improves. At the critical field [ $\mu_0 H_{cr} \approx 3.5T$ , see Fig. 6(c)], the temperature dependence of  $\rho(T)$  substantially deviates from a quadratic behaviour, thereby referring to a field-driven nFl state.

Characteristic temperatures derived from the pressure dependent resistivity study of  $\text{Yb}_2\text{Pd}_2\text{Sn}$  are summarized in Fig. 7. The magnetically ordered region is presumed to extend from approximately 1 to below 4 GPa; no magnetic order is found at 0.3 GPa and for the runs performed at 4 and 5 GPa. For the latter values a maximum in  $\rho(T, p)$  is found at

These characteristic temperatures are shown in Fig. 7, too.  $T_{\rho}^{\max}(p)$  behaves antithetic with respect to  $T_N(p)$ , in line with the mutually competing scales of the RKKY interaction ( $T_{\text{RKKY}}$ ), tending to establish long range magnetic order, and

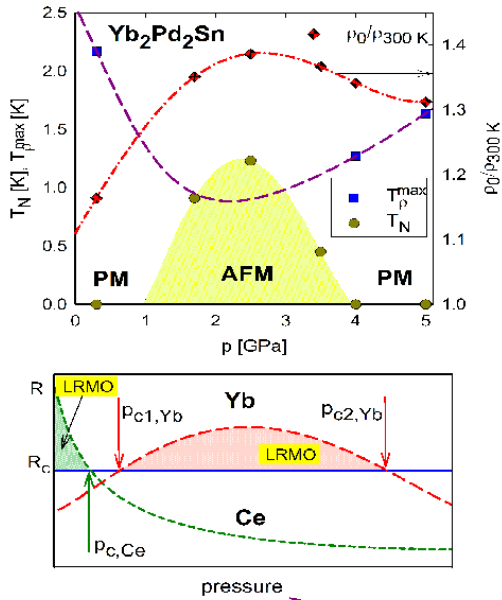


Fig. 7. Upper panel: Pressure-temperature phase-diagram of the magnetic ordering temperature (filled circles) and the low temperature resistivity maximum (filled squares) of  $\text{Yb}_2\text{Pd}_2\text{Sn}$ . The filled area sketches the phase space where long range magnetic order exists. The diamond show the pressure dependent evolution of the residual resistivity  $\rho_0$ . All lines are guides for the eye. Lower panel: Schematic pressure dependence of  $R = T_{\text{RKKY}}/T_K$  for Ce and Yb systems. The solid line shows the critical value  $R_c$  for the occurrence of QCP, thereby defining pressure ranges, where long range magnetic order (LRMO) sets in, locating the critical pressures  $p_c$  for Ce as well as  $p_{c1}$  and  $p_{c2}$  for Yb systems (sketch reproduced and modified from Ref. [19]).

the Kondo effect ( $T_K$ ), favouring a non-magnetic ground state. Within the magnetically ordered regime, the characteristic maximum in  $\rho(T)$  becomes hidden. This

relationship is quite similar to solid solution  $\text{Yb}_2\text{Pd}_2\text{In}_{1-x}\text{Sn}_x$  and mimics the concentration dependence of  $T_N$  and  $T_K$ . While for the latter case the Grüneisen parameter remains negative, a remarkable sign change of  $\Omega_K = -d(\ln T_K)/dV$  is observed as pressure augments in the case of  $\text{Yb}_2\text{Pd}_2\text{Sn}$ . That pressures where magnetic order appears or vanishes at  $T = 0$  corresponds to a QCP, and so far no other Ce or Yb based intermetallic compounds with two such QCPs have been found. Therefore,  $\text{Yb}_2\text{Pd}_2\text{Sn}$  comprises the first heavy fermion system exhibiting two pressure driven QCPs associated with magnetic ordering at  $T = 0$ .

The pressure dependent evolution of the residual resistivity  $\rho_0(p)$  is also shown in Fig. 7, evolving likewise to  $T_N(p)$ . Specifically,  $\rho_0$  adopts larger values for the phase space where magnetic ordering occurs. In general,  $\rho_0$  is governed by scattering of the conduction electrons on static imperfections of the crystal and can be expressed by  $\rho_0 = (h/e^2 l)(3\pi^2)^{1/3} N^{-2/3}$ , where  $l$  is the mean free path of the charge carriers and  $N$  is the carrier density. Since pressure does not substantially modify  $l$ , the observed increase of  $\rho_0$  corresponds to a decrease of  $N$ , perfectly matching the gap-opening scenario of antiferromagnetic order as discussed above.

The extraordinary features observed from the present pressure study of  $\text{Yb}_2\text{Pd}_2\text{Sn}$  may be understood from a novel pressure dependence of  $T_K$  uniquely derived for Yb compounds.  $T_K(p)$  results from a superposition of increasing hybridisation of  $4f$  and conduction electrons with pressure, as well as a pressure driven suppression of valence fluctuations of the Yb ion. While the latter derives from a crossover of the nonmagnetic  $4f^{14}$  electronic configuration towards the magnetic  $4f^3$  state, leading to a decreasing  $T_K$ , the former enhances  $T_K$  owing to an advanced overlap of the Yb- $4f$  wave function.

As in ordinary Kondo lattices,  $T_K(p)$  competes with the RKKY interaction,  $T_{\text{RKKY}}(p)$ , resulting in a nonmagnetic ground state for  $T_K > T_{\text{RKKY}}$ , but favouring long range magnetic order for  $T_K > T_{\text{RKKY}}$ . By defining  $R = T_{\text{RKKY}}/T_K$  a critical value  $R_c$  will be found, where the magnetic phase transition occurs at  $T = 0$ , thus the QCP of the system is approached. Owing to the peculiar U-shape like  $T_K(p)$  dependence of Yb systems, the quantum critical point of such systems at  $R = R_c$  may be crossed twice, as pressure evolves. This theoretical prediction [19], is sketched in fig. 7 and, in fact, is found experimentally for the first time in a real system,  $\text{Yb}_2\text{Pd}_2\text{Sn}$  at  $p_{c1} \approx 1$  and  $p_{c2} \approx 4$  GPa.

### 3. Summary

A pressure dependent study carried out for  $\text{Yb}_2\text{Pd}_2\text{Sn}$  revealed a novel evolution of long range magnetic order, which appears in a pressure range from roughly 1 to 4 GPa. This constitutes the possibility of two QCP, found, in fact, for the first time in a single material. The large body of Ce compounds, however, which have been studied rather intensely, never showed such a phase diagram since

both mechanisms dominating the effective Kondo interaction strength, i.e., hybridisation and valence fluctuations, are always uniformly magnified by increasing pressure. Consequently, the frequently highlighted electron - hole analogy among Ce and Yb systems is challenged, becoming rather questionable in the light of the present results.

### Acknowledgements

Work supported by the Austrian FWF, P 18054. E.B. would like to acknowledge COST P16 and Osaka University for financial support. We thank K. Miyake for many fruitful discussions. This work was also supported by MEXT.KAKENHI(15204032) and the 21st century COE Program (G18) of Japan Society for the Promotion of Science. T.M. is grateful for financial support by the 21st century COE Program.

### References

- [1] H. v. Löhneysen, A. Rosch, M. Vojta, P. Wölfle, *Rev. Mod. Phys.* **79**, 1015 (2007).
- [2] G. R. Stewart, *Rev. Mod. Phys.* **73**, 797 (2001); *Rev. Mod. Phys.* **78**, 743 (2006).
- [3] N. D. Mathur, F. M. Grosche, S. R. Julian, I. R. Walker, D. M. Freye, R. K. W. Haselwimmer, G. G. Lonzarich *Nature* **394**, 39 (1998).
- [4] S. S. Saxena, P. Agarwal, K. Ahilan, F. M. Grosche, R. K. W. Haselwimmer, M. J. Steiner, E. Pugh, I. R. Walker, S.R. Julian, P. Monthoux, G. G. Lonzarich, A. Huxley, I. Sheikin, D. Braithwaite, J. Flouquet *Nature* **406**, 587 (2000).
- [5] H. v. Löhneysen, J. Magn. Magn. Mat. **200**, 532 (1999).
- [6] D. Jaccard, K. Behnia, J. Sierro, *Phys. Lett.* **5-6**, 475 (1992).
- [7] H. Hegger, C. Petrovic, E. G. Moshopoulou, M. F. Hundley, J. L. Sarrao, Z. Fisk, J. D. Thompson, *Phys. Rev. Lett.* **84**, 4986 (2000).
- [8] N. Kimura, K. Ito, K. Saitoh, Y. Umeda, H. Aoki, T. Terashima: *Phys. Rev. Lett.* **95**, 247004 (2005).
- [9] K. Alami-Yadri, H. Wilhelm, D. Jaccard, *Eur. Phys. J. B* **6**, 5 (1998).
- [10] H. Winkelmann, M. M. Abd-Elmeguid, H. Micklitz, J. P. Sanchez, P. Vulliet, K. Alami-Yadri, D. Jaccard, *Phys. Rev. B* **60** (1999) 3324.
- [11] G. Knebel, D. Braithwaite, G. Lapertot, P. C. Canfield, J. Flouquet, *J. Phys., Condens. Matter.* **13**, 10935 (2001).
- [12] H. Winkelmann, M. M. Abd-Elmeguid, H. Micklitz, J. P. Sanchez, C. Geibel, F. Steglich, *Phys. Rev. Lett.* **81**, 4947 (1998).
- [13] J. M. Mignot, J. Wittig, In *Valence Instabilities* edited by P. Wachter and H. Boppert (North-Holland, Amsterdam, 1982), p 203. (1982).
- [14] J. Custers, P. Gegenwart, H. Wilhelm, K. Neumaier, Y. Tokiwa, O. Trovarelli, C. Geibel, F. Steglich, C. Pepin and P. Coleman, *Nature* **424**, 524 (2003).
- [15] E. Bauer, *Adv. Phys.* **40**, 417 (1991).
- [16] E. Bauer, R. Hauser, A. Galatanu, H. Michor, and G. Hilscher J. Sereni, M. G. Berisso, P. Pedrazzini M. Galli, F. Marabelli and P. Bonville *Phys. Rev. B* **60**, 1238 (1999).
- [17] E. Bauer, G. Hilscher, H. Michor, Ch. Paul, Y. Aoki, H. Sato, D. T. Adroja, J-G Park, P. Bonville, C. Godart, J. Sereni, M. Giovannini, A. Saccone, *J. Phys., Condens. Matter* **17**, S999 (2005).
- [18] D. Cox, N. Grewe, *Z. Phys. B* **71**, 321 (1988).
- [19] A. V. Goltsev, M. M. Abd-Elmeguid, *J. Phys., Condens. Matter.* **17**, S813 (2005).
- [20] K. Shimizu, K. Amaya, N. Suzuki, *J. Phys. Soc. Jpn.* **74**, 1345 (2005).
- [21] R. Lübbers, J. Dumschat, G. Wortmann, E. Bauer *J. Physique IV*, **7 C2**, 1021 (1997).
- [22] M. E. Fisher, J. S. Langer, *Phys. Rev. Lett.* **20**, 665 (1968).
- [23] Meaden *Contemp Phys.* **12**, 313 (1971)

\*Corresponding author: bauer@ifp.tuwien.ac.at